

Yeasts collectively extend the limits of habitable temperatures by secreting glutathione

Laman Trip, Diederik S.; Youk, Hyun

DOI

[10.1038/s41564-020-0704-2](https://doi.org/10.1038/s41564-020-0704-2)

Publication date

2020

Document Version

Accepted author manuscript

Published in

Nature Reviews Microbiology

Citation (APA)

Laman Trip, D. S., & Youk, H. (2020). Yeasts collectively extend the limits of habitable temperatures by secreting glutathione. *Nature Reviews Microbiology*, 5(7), 943-954. <https://doi.org/10.1038/s41564-020-0704-2>

Important note

To cite this publication, please use the final published version (if applicable). Please check the document version above.

Copyright

Other than for strictly personal use, it is not permitted to download, forward or distribute the text or part of it, without the consent of the author(s) and/or copyright holder(s), unless the work is under an open content license such as Creative Commons.

Takedown policy

Please contact us and provide details if you believe this document breaches copyrights. We will remove access to the work immediately and investigate your claim.

1 **Yeasts collectively extend the limits of habitable temperatures by**
2 **secreting glutathione**

3

4

5 Diederik S. Laman Trip^{1,2} and Hyun Youk^{1,2,3,*}

6

7

8 ¹Kavli Institute of Nanoscience,

9 ²Department of Bionanoscience, Delft University of Technology, Delft 2628CJ, The Netherlands

10 ³CIFAR, CIFAR Azrieli Global Scholars Program, Toronto ON M5G 1M1, Canada

11 *Corresponding author. Email: h.youk@tudelft.nl

12

13

14 **SUMMARY**

15

16 **The conventional view is that high temperatures cause microbes to replicate slowly or die.**
17 **In this view, microbes autonomously combat heat-induced damages. Yet, microbes co-**
18 **exist with each other, raising the underexplored and timely question of whether microbes**
19 **can cooperatively combat heat-induced damages at high temperatures. Here we use the**
20 **budding yeast, *Saccharomyces cerevisiae*, to show that cells can help each other and their**
21 **future generations survive and replicate at high temperatures. As a surprising**
22 **consequence, even for the same temperature, a yeast population can either exponentially**
23 **grow, never grow, or grow after unpredictable durations (hours-to-days) of stasis,**
24 **depending on its population density. Through the same mechanism, yeasts collectively**
25 **delay and can eventually stop their approach to extinction, with higher population-**
26 **densities stopping faster. These features arise from yeasts secreting and extracellularly**
27 **accumulating glutathione - a ubiquitous heat-damage-preventing antioxidant. We show**
28 **that secreting glutathione, which eliminates harmful extracellular chemicals, is both**
29 **necessary and sufficient for yeasts to collectively survive high temperatures. A**
30 **mathematical model, generally applicable to any cells that cooperatively replicate by**
31 **secreting molecules, recapitulates all these features. Our study demonstrates how**
32 **organisms can cooperatively define and extend the boundaries of life-permitting**
33 **temperatures.**

34

35 Microbes live in a range of “habitable temperatures” (1-3). The conventional view is that increasing
36 the temperature above some optimal value causes microbes to take more time to self-replicate
37 and that once the temperature goes beyond the habitable range - into an “unlivable temperature”
38 regime - microbes cannot replicate and they die (1-4) (Figs. 1a-b). In this textbook view, a
39 microbe's ability to replicate at high temperatures hinges on whether the cell can combat heat-
40 induced damages by itself such as misfolded proteins (5-8) which it cannot at sufficiently high
41 temperatures, leading to its death (Fig. 1c). Yet a microbe often lives with other cells instead of
42 alone, enabling them to work together for their collective survival (9-13). Given the timeliness of
43 understanding how the rising global temperatures affect organisms, we used the budding yeast,
44 *Saccharomyces cerevisiae*, to re-examine the conventional picture - one in which yeasts
45 autonomously combat heat shocks - to investigate whether microbes can also collectively combat
46 high temperatures to avoid becoming extinct (Fig. 1d).

47
48 As our starting point, we reproduced the well-known, textbook picture of how temperature
49 affects microbial growths by measuring the population-level growth rates for a laboratory-standard
50 (“wild-type”) strain of haploid budding yeast in liquid cultures (4, 14-16) (Fig. 1b and Supplementary
51 Fig. 1). In this picture, the population growth-rate is zero for temperatures of 40 °C and higher
52 (Fig. 1b and Supplementary Fig. 1). Despite being evidently true - as we reproduced it here - we
53 discovered that this textbook picture (Fig. 1c) is misleading and requires a revision. In this paper,
54 we revise this picture with experiments and a mathematical model, which reveal that, at sufficiently
55 high temperatures, yeasts secrete and extracellularly accumulate glutathione - a major antioxidant
56 for many species - that cleanses the extracellular environment of harmful reactive oxygen species
57 whose high reactivity is damaging for cells. Thus, we discovered that yeasts help each other and
58 their future generations replicate, survive, and avoid becoming extinct at high temperatures (Fig.
59 1d). In short, our work demonstrates the habitability of a temperature for a single-celled organism
60 emerging as a community-level property, determined by interactions among the members of the
61 microbial community.

62
63

64 **RESULTS**

65 **Population-density determines replicability of cells and habitability of temperature**

66 We re-examined the conventional, cell-autonomous picture by incubating populations of wild-type
67 yeasts in liquid media at a conventionally-defined habitable temperature (~38 °C), unlivable
68 temperature (~40 °C), and a transition temperature in between the two (~39 °C). This time, and

69 in contrast with the conventional picture (Supplementary Fig. 1), we precisely set the initial
70 population-density (# of cells/mL) and studied its effect on population growth. With a flow
71 cytometer, we counted the integer numbers of cells per volume to determine the population-
72 density over time. These experiments revealed surprising behaviors. Specifically, at the
73 supposedly-habitable temperature of $\sim 38^{\circ}\text{C}$, none of the replicate populations that started with a
74 relatively low population-density (200 cells/mL) grew at all during ~ 12 days of incubation except
75 for a small, transient growth that occurred for a few hours right after the transfer from 30°C (Fig.
76 2a - red curves). At the same temperature ($\sim 38^{\circ}\text{C}$), setting the initial population-density to be just
77 five times larger (1,000 cells/mL) yielded a population whose behavior was completely
78 unpredictable: it could either grow until it reached the carrying capacity (i.e., $\sim 10^7$ cells/mL) or not
79 grow at all after the initial transient-growth (Fig. 2a - green curves). When the population did grow,
80 it could wait four days or eight days or some other, unpredictable time before starting to grow (Fig.
81 2a - multiple green curves). Still, at the same temperature ($\sim 38^{\circ}\text{C}$), setting the initial population-
82 density to be again just five times larger (5,000 cells/mL) yielded populations that always grew
83 exponentially and identically over time up to the carrying capacity (Fig. 2a - blue curves). Thus, at
84 the supposedly "habitable" temperature of 38°C , only the largest of the three initial population-
85 densities led to the deterministic growth that the conventional picture states should be exhibited
86 by every population (1,14-16). The same three, population-density-dependent growth behaviors
87 also occur near the upper limit of the habitable temperatures ($\sim 39^{\circ}\text{C}$) (Fig. 2b). Moreover, we
88 found that populations with sufficiently many cells can grow at $\sim 40^{\circ}\text{C}$ - a supposedly "unlivable"
89 temperature (Fig. 2c - non-red curves). These results show that in order to determine whether a
90 yeast-population grows or not, one must know *both* the temperature and the initial population-
91 density.

92

93 **Phase diagram summarizes population-level behaviors across temperatures**

94 By incubating liquid cultures of populations with differing initial densities at multiple temperatures,
95 we constructed a "phase diagram" (Fig. 2d and Supplementary Figs. 3-4). The phase diagram,
96 summarizing the population-level growth behaviors, consists of four phases - deterministic growth,
97 random growth, no-growth, and no-growth due to insufficient nutrients - as a function of the initial
98 population-density and temperature. It reveals that the conventional picture (Figs. 1b-c) mistakenly
99 arises because one typically sets the initial population-density to lie within some narrow range
100 when studying population growths. This leads to, for example, the growth rate *appearing* to
101 decrease as the temperature increases within a given range (e.g., $36.5^{\circ}\text{C} \sim 39^{\circ}\text{C}$) (Fig. 1b). But,
102 in fact, for the same temperature range, we found that the populations' growth rates - when they

103 grew - were poorly correlated with temperature and could highly vary among populations even for
104 the same temperature if we widely varied the initial population-density (Fig. 2e). The phase
105 boundary between the deterministic-growth and random-growth phases (Fig. 2d) describes the
106 minimum, initial population-density necessary to guarantee that a population grew at each
107 temperature. Conversely, the phase boundary between the random-growth and no-growth phases
108 (Fig. 2d) describes the maximum, initial population-density necessary to guarantee that a
109 population never grew at each temperature. Both of these values are highly sensitive to
110 temperature (e.g., a ~100-fold change when going from 39 °C to 40 °C (Fig. 2d)). The random-
111 growth phase may be seen as a hybrid of the deterministic-growth and no-growth phases. A small
112 change of either can transform a no-growth into a deterministic-growth and vice-versa (Fig. 2a).
113 Intriguingly, all phase boundaries converge at a single point ("fold-bifurcation point") located at
114 40.3 °C, leading to only the no-growth phase at temperatures beyond 40.3 °C (Fig. 2d).
115 Specifically, at temperatures higher than 40.3 °C, populations can grow but stop growing before
116 reaching the carrying capacity, with their final population-densities depending on their initial
117 population-densities. The term, "fold-bifurcation point" comes from dynamical systems theory and
118 is the point in the phase diagram where a stable fixed point (carrying capacity) merges with an
119 unstable fixed point (the upper boundary of the no-growth phase).

120

121 **Expressing a superfluous gene reshapes phase diagram**

122 We discovered that forcing yeasts to constitutively express the Green Fluorescent Protein (GFP),
123 which serves no function for cell growth, shifts the phase boundaries (Fig. 2f and Supplementary
124 Fig. 5). In particular, reducing the GFP expression could shift the phase boundaries by several
125 degree Celsius, suggesting that the cost of expressing superfluous genes can markedly alter the
126 phase diagram. In light of previous studies (17,18), this may be due to expressing GFP shifting
127 the intracellular resources, which may be especially crucial for surviving high temperatures, away
128 from performing roles that are for cell growth. While our study has revealed a genetic means for
129 reshaping the phase diagram, the molecular mechanisms that underlie the reshaping are left for
130 future studies.

131

132 **A few cells initiate population growth in random-growth phase and transiently replicating** 133 **sub-populations exist in non-growing populations**

134 We turned to single-cell-level measurements for further insights. The wild-type strain has a
135 mutated *ade2* gene that causes a cell to accumulate a red pigment, which can only be diluted by
136 persistent cell divisions (19). Thus, we could use our flow cytometer's red-fluorescence detector

137 to determine which cells had been replicating and which cells had not (Extended Data Fig. 1). For
138 a deterministically growing population, we discovered that, after a short transient growth
139 associated with the transfer from 30 °C to the high temperature, the number of replicators
140 exponentially increased over time up to the carrying capacity (Extended Data Fig. 1). In contrast,
141 for random-growth and no-growth populations, the number of replicators typically decreased until
142 very few cells (~1-5% of population) remained as replicators. Subsequently, the number of
143 replicators either spontaneously increased by orders of magnitude after an unpredictable hours or
144 days (random-growth) or remained sustainably low and fluctuated by few-folds over nearly a week
145 (no-growth) (Extended Data Fig. 1). These fluctuations were sufficiently small that the total
146 population-density remained nearly constant. These results establish that a small sub-population
147 of transiently replicating cells exist and that the fraction of replicators in the population could stably
148 remain in low numbers (e.g., ~1% of total population). We will later return to these features with a
149 mathematical model that recapitulates them.

150

151 **Cells collectively combat extinctions at high temperatures**

152 We next asked whether cell death, like cell replication, also depends on the initial population-
153 density. At several temperatures, we measured how the number of surviving cells changed over
154 time for no-growth phase populations (Supplementary Fig. 6). Surprisingly, these measurements
155 deviated qualitatively, not just quantitatively, from the textbook picture in which microbes such as
156 yeasts autonomously die and that dictates that the number of survivors should exponentially
157 decrease over time (4) (Fig. 3a - brown line). Yet, we discovered that the number of survivors
158 decreases over time in a heavy-tailed (power-law-like) manner (Fig. 3a - blue curve). In other
159 words, the population continuously decelerates, and eventually would cease, its approach to
160 extinction. For example, after three days at 41 °C, the number of survivors in a population deviated
161 by $\sim 10^7$ -fold from the expected value dictated by the conventional theory (Fig. 3a - last time point;
162 Supplementary Figs. 6). Moreover, we discovered that the rate at which cells die at high
163 temperatures depends on the initial population-density (Fig. 3b and Supplementary Fig. 6).
164 Specifically, the number of survivors appears to exponentially decrease during the first day before
165 it noticeably enters a heavy-tailed decay regime on later days (Fig. 3b). Hence, we can assign a
166 constant rate of decay to each population to describe how the number of survivors initially
167 decreases (e.g., during the first day at a high temperature). We found that this rate ("initial death-
168 rate") decreases as the initial population-density increases, meaning that the number of survivors
169 decreases more slowly for higher initial population-densities (Fig. 3b - three dashed lines). These
170 results suggest a highly non-linear, cooperative effect that cells have on each other's survival.

171
172 **Temperature of the fold-bifurcation point separates two extinction-avoidance regimes**
173 We next measured the initial death-rate at multiple temperatures for populations of differing initial
174 densities. The population half-life, which is derived from the initial death-rate and is the time taken
175 for the number of survivors to be halved, should be independent of the initial population-density,
176 according to the conventional view in which yeasts autonomously die (Fig. 3c). Instead, we
177 discovered that increasing the initial population-density always increases the population half-life
178 and that the temperature determines how sensitively the population half-life depends on the initial
179 population-density (Fig. 3d). Specifically, a population half-life has two regimes of sensitivities.
180 Temperatures below 40.3 °C exhibit the first regime. Here the population half-life is highly
181 sensitive to the initial population-density: it increases from hours to days if the initial population-
182 density nearly doubles (Fig. 3d - yellow curves for 39 °C ~ 40 °C). Moreover, as the initial
183 population-density keeps increasing, the population half-life keeps increasing and eventually
184 becomes infinity. This is because a sufficiently high-density population grows at these
185 temperatures (Fig. 2d). Temperatures above 40.3 °C exhibit the second regime: increasing the
186 initial population-density above some value hardly changes the population half-life, which
187 eventually plateaus at a finite value as the initial population-density keeps increasing (Fig. 3d -
188 purple curves for 41 °C ~ 43 °C). This occurs because populations cannot grow regardless of
189 their initial densities at these temperatures (Fig. 2d). At the fold-bifurcation point (Fig. 2d), the
190 population-density can remain at a nearly constant value (i.e., population half-life is infinite
191 because the initial death-rate is zero). The fold-bifurcation point is the only place in the phase
192 diagram (at 40.3 °C with $\sim 1 \times 10^5$ cells/mL) at which a non-growing population's half-life is infinite.
193 In other words, a population at the fold-bifurcation point can constantly maintain its density,
194 apparently indefinitely, unless fluctuations cause its demise. Taken together, our results establish
195 that a yeast's death depends on the other cells in the population. Moreover, we determined that
196 neither heat-resistant mutants nor "persister-like" cells such as those seen in antibiotic persistence
197 (20) can explain our data on cell deaths (Extended Data Fig. 2).

198
199 **Extracellular factor dictates cell replications at high temperatures**
200 We next sought to uncover the mechanisms that underlie the density-dependent replications and
201 deaths of yeasts. As a start, we determined that cells isolated from a growing culture and put into
202 a fresh medium do not grow, whereas the liquid medium isolated from an exponentially growing
203 population and transplanting a fresh population of cells into it causes that population to grow, even
204 though the phase diagram indicated that the population initially had too few cells for it to grow (Fig.

205 4a-c, Supplementary Figs. 7-8). These results suggested that an “instruction” that dictates
206 population growths resides in the extracellular - not intracellular - environment. Moreover, we
207 confirmed that depletion of any of the nutrients does not instruct a population to grow
208 (Supplementary Figs. 8-9), indicating that it is the secretion of some factor(s) at high temperatures
209 that induces population growths.

210

211 **Yeasts secrete glutathione to help each other replicate at high temperatures**

212 By performing a transcriptome analysis (RNA-seq) on wild-type yeasts at different locations in the
213 phase diagram (Supplementary Fig. 10), we uncovered gene-expression profiles that are similar
214 to those of yeasts undergoing environmental stresses (21,22). We hypothesized that yeasts at
215 high temperatures may be stressed due to reactive oxygen species, which are known to be
216 abundant at high temperatures (23-25) and damaging for cells (26-28). Given that antioxidants
217 inactivate reactive oxygen species, we further hypothesized that yeasts at high temperatures may
218 be secreting antioxidants. Indeed, studies have found that heat-shocked yeasts produce and
219 maintain elevated levels of intracellular glutathione (23,24), a tripeptide that is the yeast's primary
220 antioxidant (23,29,30) besides having other essential roles (31). Although much is known about
221 glutathione's intracellular roles in yeast (29-34), little is known about whether yeasts secrete
222 glutathione and, if so, why and when they would do so aside from a few examples such as yeasts
223 secreting glutathione to defend against harmful extracellular arsenite (35).

224 Supporting our hypothesis, is the fact that yeasts are known to secrete small amounts of
225 glutathione in stationary-phase at 30 °C (after diauxic shift) (36), and that we found that medium
226 coming from such populations induces growth at high temperatures (Supplementary Fig. 8).
227 Indeed, we discovered that adding high concentrations of either glutathione or ascorbic acid - both
228 antioxidants (29) - to the growth medium caused growth of populations that, without the added
229 antioxidants, could not have grown by themselves because they had too few cells (Fig. 4d). Hence,
230 extracellular antioxidants - glutathione and ascorbic acids - are sufficient for inducing yeast-
231 population growths at high temperatures. Focusing on glutathione, we found that random-growth
232 phase and deterministic-growth phase populations continuously secreted and extracellular
233 accumulated glutathione during log-phase growths and stationary-phase at high temperatures
234 (Fig. 4e and Supplementary Fig. 11). But we detected only small concentrations of extracellular
235 glutathione that barely increased over time for no-growth phase populations at high temperatures.
236 Moreover, consistent with the population-density dependent growths only occurring for
237 temperatures above ~36 °C being caused by glutathione, we found that yeasts secreted
238 glutathione only at temperatures above ~36 °C but not below it (Fig. 2d and Supplementary Fig.

239 11). Furthermore, we had to add sufficiently high concentrations of glutathione to induce growth
240 of a population that could not grow by itself (Fig. 4f). Specifically, if the extracellular glutathione
241 concentration was below $\sim 0.3 \mu\text{M}$, populations hardly grew. But extracellular glutathione
242 concentrations above $\sim 0.3 \mu\text{M}$ induced population growths up to carrying capacity. Consistent
243 with these findings, when we did not add any glutathione at high temperatures, no-growth
244 populations had accumulated less than $\sim 0.3 \mu\text{M}$ of extracellular glutathione whereas the growing
245 population had accumulated more than $\sim 0.3 \mu\text{M}$ of extracellular glutathione (Fig. 4d). In summary,
246 we have now established that yeasts at high temperatures secrete and extracellularly accumulate
247 glutathione that - above some threshold concentration ($\sim 0.3 \mu\text{M}$) - induces population growths
248 (Fig. 4g).

249

250 **Mathematical model recapitulates experimental data**

251 To explain our data, we developed a stochastic, mathematical model that contained just one free
252 parameter (see Supplementary text). In this model, each alive cell secretes glutathione at a
253 constant rate and in each time step, with some probability, takes one of three actions: replicate,
254 die or stay alive without replicating (Fig. 5a). The probability of dying is fixed by and linearly
255 increases with temperature. Given that yeast-populations require at least a threshold glutathione-
256 concentration for growth (Fig. 4f), the probability of replicating non-linearly increases with
257 extracellular glutathione concentration in our model (Fig. 5b). The only free parameter, which
258 requires fitting to our data, is the extracellular glutathione concentration at which the probability of
259 replicating is half its maximum (Fig. 5b - blue curve). All other parameters are directly read-off
260 from our data (Supplementary text).

261 Our model recapitulates all the main experimental data (Figs. 5c-f and Extended Data Fig.
262 3). The model's main idea is that in order to avoid becoming extinct at a high temperature, the
263 population - which initially lacks any extracellular glutathione and thus starts with a zero probability
264 of a cell replicating - must keep accumulating extracellular glutathione to keep increasing the
265 probability of replication up to and above the probability of a cell dying - which is fixed by the
266 temperature (Extended Data Fig. 3). Populations achieve this if and only if they starts with
267 sufficiently many cells. Populations with too few cells goes extinct and belong to the no-growth
268 phase because they have insufficient time to accumulate enough extracellular glutathione: the
269 probability of replicating increases until the last cell dies but always remains below the probability
270 of dying. Populations with intermediate densities may grow or approach extinction (i.e., exhibits
271 the random-growth phase) because the glutathione concentration nears the threshold
272 concentration by the time there are very few surviving cells, whose stochastic replications or

273 deaths subsequently determine whether or not the probability of replicating exceeds that of dying.
274 At temperatures above ~ 40.3 °C - where the fold-bifurcation is - the probability of dying exceeds
275 the maximally allowed probability of replicating, meaning that only the no-growth phase is possible
276 at these temperatures (Fig. 5b – grey dashed line). In the no-growth phase, the continuous
277 accumulation of extracellular glutathione results in populations decelerating their approach to
278 extinction over time, leading to the heavy-tailed function describing the number of survivors
279 decreasing over time and populations with higher initial densities more slowly approaching
280 extinction (see Supplemental Fig. 12). Taken together, our minimal model recapitulates all the
281 main experimental data (Figs. 5c-f).

282

283 **Extracellular glutathione is necessary and sufficient for surviving high temperatures**

284 To address whether extracellular glutathione is necessary - not only sufficient (Fig. 4e-f) - for
285 yeasts to survive high temperatures, we used a "masking reagent" (1-Methyl-2-vinylpyridinium,
286 M2VP) that specifically inactivates extracellular glutathione only, without interfering with the
287 intracellular glutathione and any other processes (Supplementary Fig. 13) (37,38). Adding the
288 masking agent stopped deterministically growing populations at high temperatures (Fig. 6a). Thus,
289 glutathione is both necessary and sufficient - glutathione is the only responsible molecule - for
290 inducing cell replications at high temperatures (above ~ 36.7 °C).

291

292 **Manipulating synthesis, import, and export of glutathione at high temperatures**

293 To gain further insights, we constructed mutants that were either unable to synthesize glutathione
294 (*gsh1Δ*-strain) (Fig. 6b) (39), or unable to import glutathione (i.e., *hgt1Δ*-strain) (40), or had
295 severely reduced ability to secrete glutathione (*gex1,2Δ-adp1Δ*-strain) (41,42). We found that the
296 mutants that cannot synthesize glutathione (*gsh1Δ*-strain) confirmed our earlier conclusion that
297 the wild-type cells secrete glutathione only at high temperatures (above ~ 36 °C) (Extended Data
298 Fig. 4). We also found that the mutants that cannot import glutathione (*hgt1Δ*-strain) have the
299 same population-density-dependent growths at high temperatures as the wild-type strain (Fig. 6c).
300 Thus, yeasts do not need to import extracellular glutathione in order to replicate at high
301 temperatures. This, in turn, means that glutathione's extracellular action alone, not intracellular
302 action, is responsible for promoting replications at high temperatures. Indeed, we found that the
303 mutants with significantly reduced abilities to secrete glutathione (*gex1,2Δ-adp1Δ*-strain) are less
304 able to replicate than the wild-type strain (Fig. 6d), thus requiring a higher initial population-density
305 for growth. Consistent with glutathione's extracellular action – rather than intracellular action –
306 promoting cell replications, we found that reducing the export of glutathione reduces the

307 populations' ability to grow at high temperatures. Strikingly, we found that the mutants with a
308 reduced glutathione-export (*gex1,2Δ-adp1Δ*-strain) still secreted measurable amounts of
309 glutathione at high temperatures, which is not due to glutathione passively leaking out through cell
310 membranes, meaning that other glutathione exporters function at high temperatures.

311

312 **Yeasts can replicate at “unlivable” temperatures**

313 No population can avoid extinctions at temperatures higher than 40.3 °C (Fig. 2d) because the
314 cells die too fast to accumulate enough extracellular glutathione. Hence, giving high
315 concentrations of glutathione to populations at the start of incubation at extremely high
316 temperatures may help them accumulate enough glutathione before extinction. Indeed, at 41 °C
317 for example, we could rescue populations with as low as 400 cells/mL from extinction: they
318 exponentially grow until reach a carrying capacity (Fig. 6e).

319

320

321 **DISCUSSION**

322 By showing that secreting and extracellularly accumulating glutathione is necessary and sufficient
323 for yeasts and their future generations to survive and replicate at high temperature (Fig. 6f), our
324 work revises the textbook view of cells autonomously combating heat-induced damages. A
325 common explanation for why cells, including budding yeasts, cannot replicate at high temperatures
326 is that essential proteins unfold at high temperatures (6). Our work suggests that this explanation
327 requires revisions. In fact, we found that yeasts with enough extracellular glutathione can replicate
328 at extremely high temperatures for which such proteins would unfold (i.e. above 41 °C - Fig. 6e,
329 Supplementary Fig. 12). Glutathione, an antioxidant essential for many organisms, including
330 humans (29), is central to diverse processes (30-35). Our work extends the relatively little-known
331 extracellular functions of glutathione in yeast (35,36,43) by showing that yeasts must secrete
332 sufficient amounts of glutathione at high temperatures during log-phase growth and stationary
333 phases. We found that the glutathione extracellularly accumulates and that either ~75% (for no-
334 growth populations) or ~25% (for growing populations) of it exists in in the oxidized form
335 (Supplementary Fig. 11). Both values, 75% and 25%, are higher than the previously reported
336 values for oxidized glutathione that budding yeasts steadily maintain (36), suggesting that yeasts
337 collectively "clean up" their environment by reducing harmful, extracellular reactive oxygen
338 species and thereby help each other and their future generations replicate and survive high
339 temperatures.

340 Researchers have observed fold-bifurcation points, like the one in our study (Fig. 2d), in
341 other microbial populations on the verge of extinctions such as those in which yeasts collectively
342 hydrolyze extracellular sucrose (44-46). These dynamical systems, including ours, typically exhibit
343 features familiar from phase transitions such as “critical slowing down” (45) which, in our study,
344 manifests as the yeast-population’s half-life being infinite at the fold-bifurcation point (Fig. 3d). By
345 uncovering a phase diagram for cell replication, our work may aid in advancing theories of non-
346 equilibrium statistical mechanics (47) that pertain to biologically realistic, self-replicating systems
347 that drive and maintain themselves out of thermal equilibrium. Moreover, investigating how
348 organisms can collectively combat high temperatures, as in our study, may suggest ways to help
349 organisms combat climate change and help us understand how climate change impacts unicellular
350 life and multicellular communities.

351

352 **Methods**

353

354 **Growth media and strains.** The "wild-type", haploid yeast strain that we used is from Euroscarf
355 with the official strain name "20000A". It is isogenic to another laboratory-standard haploid yeast
356 "W303a", and has the following genotype: *MATa*; *his3-11_15*; *leu2-3_112*; *ura3-1*; *trp1Δ2*; *ade2-*
357 *1*; *can1-100*. We built the two strains that constitutively expressed GFP by first using PCR to insert
358 a functional *ADE2* gene into the locus of the defective *ade2* gene in the wild-type strain, by a
359 homologous recombination, so that the red pigments that would have accumulated without the
360 *ADE2* insertion no longer existed (i.e., the strain can now synthesize adenine). We could thus
361 detect their GFP fluorescence without interferences from the red pigments. After replacing the
362 defective *ade2* locus with a functional *ADE2*, we constructed the 1x-GFP and 100x-GFP strains
363 (see GFP-expression levels in Supplementary Fig. 5a) by integrating a single-copy of an
364 appropriate, linearized yeast-integrating plasmid at the *his3* locus on the chromosome.
365 Specifically, the 1x-GFP strain had its GFP expression controlled by the constitutive promoter of
366 yeast's *KEX2* gene (621 bases upstream of its ORF) which was on a yeast-integration plasmid
367 (48) that constitutively expressed *HIS3* (from *C. glabrata*) and integrated into the non-functional
368 *his3* locus of the wild-type strain by a homologous recombination. The 100x-GFP strain had its
369 GFP expression controlled by a strong constitutive promoter pGPD1 (48) which was on the same
370 plasmid as the one for the 1x-GFP strain except that the *KEX2* promoter was swapped with the
371 *GPD1* promoter. We cultured all yeasts in defined, minimal media that consisted of (all from
372 Formedium): Yeast Nitrogen Base (YNB) media, Complete Supplement Mixture (CSM) that
373 contained all the essential amino acids and vitamins, and glucose at a saturating concentration
374 (2% = 2 g per 100 mL). The agar pads, which we used for growing yeast colonies, contained 2%-
375 agar (VWR Chemicals), Yeast Extract and Peptone (YEP) (Melford Biolaboratories Ltd.), and a
376 2%-glucose.

377

378 **Growth experiments.** In a typical growth experiment, we first picked a single yeast colony from
379 an agar plate and then incubated it at 30 °C for ~14 hours in 5 mL of minimal medium, which
380 contained all the essential amino acids and a saturating concentration of glucose (2%).
381 Afterwards, we took an aliquot of a defined volume from the 5 mL culture (typically 20 μL), and
382 then flowed it through a flow cytometer (BD FACSCelesta with a High-Throughput Sampler) to
383 determine the 5 mL culture's population-density (# of cells/mL). We then serially diluted the culture
384 into fresh minimal media to a desired initial population-density for a growth experiment at various

385 temperatures. Specifically, we distributed 5-mL of diluted cells to individual wells in a "brick" with
386 twenty-four 10 mL-wells (Whatman: "24-well x 10mL assay collection & analysis microplate"). This
387 ensured that we had 8 identical replicate cultures for each initial population-density (e.g., in Figure
388 2a-c). We sealed each brick with a breathable film (Diversified Biotech: Breathe-Easy), covered it
389 with a custom-made Styrofoam-cap for insulation, and incubated it in a compressor-cooled, high-
390 precision thermostatic incubators (Memmert ICP260) that stably maintained their target
391 temperature throughout the course of our growth-experiments, with a typical standard deviation of
392 0.017 °C over time (deviation measured over several days - see Supplementary Fig. 2).
393 Throughout the incubation, the cultures in the brick were constantly shaken at 400 rpm on a plate
394 shaker (Eppendorf MixMate) that we kept in the incubator. To measure their population-densities,
395 we took a small aliquot (typically 50 μ L) from each well, diluted it with PBS (Fisher Bioreagents)
396 into a 96-well plate (Sarstedt, Cat. #9020411), and then flowed it through the flow cytometer which
397 gave us the # of cells/mL. We determined the growth rates by measuring the maximum slope of
398 the log-population-density after their initial, transient growths.

399

400 **Flow cytometry.** We used BD FACSCelesta with a High-Throughput Sampler and lasers with the
401 following wave lengths: 405 nm (violet), 488 nm (blue), and 561 nm (yellow/green). We calibrated
402 the FSC and SSC gates to detect only yeast cells (FSC-PMT=681V, SSC-PMT=264V, GFP-
403 PMT=485V, mCherry-PMT=498V. As a control, flowing PBS yielded no detected events). The
404 number of cells per mL that we plotted in our growth experiments is proportional to the number of
405 events (yeast cells) that the flow cytometer measured in an aliquot of cells with a defined volume.
406 We measured the GFP fluorescence with a FIT-C channel and the "red cells" (Extended Data Fig.
407 1) with a mCherry channel. We analysed the flow cytometer data with a custom MATLAB script
408 (MathWorks).

409

410 **Measuring number of surviving cells.** For Figures 3a-b, Extended Data Fig. 2 and
411 Supplementary Fig. 6, we prepared 250 mL cultures of wild-type cells in 500 mL Erlenmeyer
412 flasks. We placed a constantly spinning magnetic stir-bar at the bottom of the flasks and placed
413 each flask on top of spinning magnets (Labnet Accuplate - at 220 rpm) inside the thermostatic
414 incubators (Memmert ICP260) that we set at desired high temperatures. For Figure 3d, we
415 prepared a brick with cultures as described in the "Growth Experiments" section in order to have
416 multiple replicate populations and to compare the different population-densities. For every time

417 point we ensured that these populations were not growing (i.e., all populations were in the no-
418 growth phase after a transient growth) by using the flow cytometer to measure their population-
419 densities over time to verify that their population-densities indeed remained constant over time.
420 For the first 48 hours of incubation, we measured the number of Colony Forming Units (CFUs) by
421 taking out a small volume aliquot from the liquid cultures at high temperatures and distributed
422 droplets from a serial dilution of the aliquot across an agar pad (2% glucose with YEP) that we
423 then incubated in 30 °C for several days until (no) colonies appeared. When there were few
424 surviving cells per mL - especially for the last time points in each experiment - we determined, in
425 parallel to the plating method, the number of CFUs by transferring an appropriate volume of the
426 liquid cultures from the incubator to an Erlenmeyer flask and then diluting it with the same volume
427 of fresh minimal media. We sealed this flask with a breathable film (Diversified Biotech: Breathe-
428 Easy) and then left it still without stirring, on a benchtop at ~24-30 °C - we checked that slightly
429 lower temperatures (e.g., room temperatures) did not affect colony-forming abilities - which
430 allowed any surviving cells to settle down to the bottom of the flask and form colonies. We counted
431 the number of colonies at the bottom of the flask - this is the value that we plotted as the last time
432 points in each experiment (Fig. 3a, Extended Data Fig. 2 and Supplementary Fig. 6).

433

434 **Cell-transfer experiments.** We incubated a 24-well brick that contained liquid cultures, each of
435 which were in a deterministic-growth phase, at a desired temperature (e.g., 10,000 cells/mL at
436 39.2 °C). We incubated the brick containing these liquid cultures in the thermostatic incubators
437 (Memmert ICP260) as described in the "Growth experiments" section. About 48 hours after the
438 incubation, we took aliquots from the cultures that were growing in mid-log phase (as checked by
439 flow cytometry) and then diluted each of them into fresh 5 mL minimal media that were in 24-well
440 bricks so that these newly created populations were in the no-growth phase at the same
441 temperature as the original population that they came from (400 cells/mL at 39.2 °C). We sealed
442 the 24-well brick with a breathable film (Diversified Biotech: Breathe-Easy) and then incubated
443 them at the same temperature as the original population. We performed the growth experiments
444 with these new populations as described in the "Growth experiments" section.

445

446 **Medium-transfer experiments.** Details are also in Supplementary Fig. 8. At a given temperature,
447 we first grew populations in the deterministic-growth phase (e.g., initial population-density of
448 30,000 cells/mL at 39.2 °C). We used a flow cytometer to measure their growing population-

449 densities at different times so that we knew in which part of deterministic growth they were in (e.g.,
450 mid-log phase). We then transferred each liquid culture to a 50 mL tube (Sarstedt) and centrifuged
451 it so that the cells formed a pellet at the bottom of the tube. We then took the resulting supernatant,
452 without the cell pellet, and flowed it through a filter paper with 200 nm-diameter pores (VWR: 150
453 mL Filter Upper Cup) to remove any residual cells from the supernatant. After filtering, we flowed
454 an aliquot of the filtered media through a flow cytometer to verify that there were no cells left in
455 the filtered media. We incubated fresh cells into these filtered media (instead of into fresh minimal
456 media) and proceeded with a growth experiment at a desired temperature as described in the
457 "Growth experiments" section.

458

459 **Measuring the depletion of extracellular nutrients.** Details are also in Supplementary Fig. 9.
460 We prepared various growth media by diluting the minimal media (SC media) by various amounts
461 with water. These diluted SC-media were each supplemented with a 2% glucose. Next, we
462 incubated fresh cells in these diluted SC-media at the desired temperature (e.g. 39.2 °C) as
463 described in the "Growth experiments" section. We compared populations of cells that initially had
464 400 cells/mL (this corresponds to a no-growth phase, see Fig. 2d) with populations that initially
465 had 10,000 cells/mL (this corresponds to a deterministic-growth phase, see Fig. 2d) in order to
466 confirm that cells were still able to grow in these media. Similarly, we also varied the amounts of
467 glucose that we supplemented to SC-media.

468

469 **RNA-seq.** For each temperature that we studied, we collected cells in 50 mL tubes and spun them
470 in a pre-cooled centrifuge. We then extracted RNA from each cell-pellet with RiboPure Yeast Kit
471 (Ambion, Life Technologies) as described by its protocol. Next, we prepared the cDNA library with
472 the 3' mRNA-Seq library preparation kit (Quant-Seq, Lexogen) as described by its protocol.
473 Afterwards, we loaded the cDNA library on an Illumina MiSeq with the MiSeq Reagent Kit c2
474 (Illumina) as described by its protocol. We analysed the resulting RNA-Seq data as previously
475 described (49): We performed the read alignment with TopHat, read assembly with Cufflinks, and
476 analyses of differential gene-expressions with Cuffdiff. We used the reference genome for *S.*
477 *cerevisiae* from ensembl. We categorized the genes by the Gene Ontologies with AmiGO2 and
478 manually checked them with the Saccharomyces Genome Database (SGD).

479

480 **Measuring concentration of extracellular glutathione.** To quantify the concentration of
481 extracellular glutathione, cells were removed from their liquid media by flowing the liquid cultures
482 that contained cells through a 0.45 μm pore filter (VWR, cellulose-acetate membrane). To ensure
483 and verify that there were no cells remaining in the filtered media, we flowed the filtered media
484 through a flow cytometer. The flow cytometer indeed did not detect any cells in the filtered media.
485 We measured concentrations of glutathione in the filtered media as described in the
486 manufacturers' protocol (38185 quantification kit for oxidized and reduced glutathione, 200 tests).
487 We used "BMG Labtech Spectrostar Nano" to measure the optical absorbance at 415 nm. As a
488 background subtraction (blank) for all absorbance measurements, we subtracted the absorbance
489 that we obtained by applying the assay to fresh minimal medium which does not have any
490 glutathione (the background absorbance could come from, for example, cysteine in the minimal
491 media). We subsequently determined the concentrations of extracellular glutathione by using a
492 calibration curve that we constructed by measuring the absorbance at 415 nm for known amounts
493 of glutathione that we added by hand into a buffer provided by the manufacturer.

494

495 **Glutathione masking experiment.** We incubated a brick of liquid cultures that were in the
496 deterministic-growth phase (20.000 cells/mL) at 39.2 $^{\circ}\text{C}$. After some time (e.g., 8.5 hours
497 afterwards), we added 750 μM of 1-Methyl-2-vinylpyridinium (M2VP, Sigma-Aldrich Cat. No.
498 69701), which is a thiol scavenging agent that rapidly masks reduced glutathione (38) and
499 proceeded with the experiment as described in the "Growth experiments" section. Identical
500 replicate cultures, that did not receive the M2VP, were used as a reference.

501

502 **Mutant yeasts.** We constructed mutant strains that could not synthesize glutathione or could not
503 import or export glutathione. Primers were designed with a 50-60 bp sequence that was either
504 homologous to the 50-60 bp that is upstream of the desired gene's start codon or downstream of
505 the desired gene's stop codon. These primers were used to amplify a selection marker by PCR,
506 resulting in a PCR product that contained a selection marker and whose ends were homologous
507 to the flanking regions of the gene to be knocked out. The wild-type strain (W303) was grown
508 overnight in a 5 mL YPD in a rotator (40 rpm) at 30 $^{\circ}\text{C}$, and subsequently transformed with the
509 PCR fragment using standard methods of yeast cloning. The biosynthesis mutant (*gsh1 Δ* -strain)
510 was constructed by removing the *GSH1* gene from W303. The import mutant (*hgt1 Δ* -strain) was
511 constructed by removing the *HGT1* gene. The export mutant (*gex1,2 Δ -adp1 Δ* -strain) was

512 constructed by removing, sequentially, the *GEX1* gene, then the *GEX2* gene, and then the *ADP1*
513 gene. The resulting transformants were grown on YPD selection plates, and knockouts were
514 verified by PCR.

515

516 **Measuring integrity of cell membrane.** Cells of the *gex1,2Δ-adp1Δ*-strain were incubated in
517 liquid media at 39.2 °C (3,000-10,000 cells/mL; corresponds to a random-growth phase). We took
518 aliquots of these cultures and then stained them with 1 µg/mL of propidium iodide (Thermo Fisher
519 Cat. No. P3566). We then flowed these stained aliquots through a flow cytometer. The flow
520 cytometer measured the number of cells that were unstained by the propidium iodide (i.e., cells
521 whose membranes were intact).

522

523 **Mathematical model.** Derivations of equations, a detailed description of the mathematical model,
524 and the parameter values used for simulations are in the Supplemental text.

525

526 **Code availability.** All scripts used for simulations in this work are publicly available (GitHub
527 [diederikIt/YeastHighTemperatures](#)).

528

529 **Data Availability.** The authors declare that all data supporting the findings of this study are
530 available within the paper and its supplementary information files. RNA-Seq data is available at
531 NCBI GEO (accession #137151). Source data for the main figures is provided. The data that
532 support the findings of this study are available from the corresponding author upon reasonable
533 request.

534

535 **References:**

- 536 1. M. T. Madigan, J. M. Martinko, D. A. Stahl, & D. Clark. *Brock biology of microorganisms* (13th
537 Ed.) (Pearson, 2011), pp. 162-163.
- 538 2. R. Milo, & R. Phillips. *Cell biology by the numbers* (1st ed.) (Garland Science, 2015),
539 <http://book.bionumbers.org/how-does-temperature-affect-rates-and-affinities/>.
- 540 3. L. Bruslind. *Microbiology*. (Open Oregon State University, 2019),
541 <http://library.open.oregonstate.edu/microbiology/chapter/environmental-factors/>
- 542 4. P. M. Doran. *Bioprocess Engineering Principles* (2nd ed.) (Academic Press, 2012), pp. 653-
543 655.
- 544 5. K. Ghosh, & K. Dill. Cellular proteomes have broad distributions of protein stability. *Biophys J*
545 **99**:3996-4002 (2010).
- 546 6. P. Leuenberger *et al.*, Cell-wide analysis of protein thermal unfolding reveals determinants of
547 thermostability. *Science* **355**, eaai7825 (2017).
- 548
- 549 7. J. Verghese, J. Abrams, Y. Wang, & K. A. Morano. Biology of the heat shock response and
550 protein chaperones: Budding yeast (*Saccharomyces cerevisiae*) as a model system.
551 *Microbiol. Mol. Biol. Rev.* **76**:115-158 (2012).
- 552
- 553 8. K. Richter, M. Haslbeck, & J. Buchner. The heat shock response: life on the verge of death.
554 *Mol. Cell* **40**:253-266 (2010).
- 555
- 556 9. M. B. Miller, & B. L. Bassler. Quorum sensing in bacteria. *Annu. Rev. Microbiol* **55**:165-199
557 (2001).
- 558
- 559 10. J. Gore, H. Youk, & A. van Oudenaarden. Snowdrift game dynamics and facultative cheating
560 in yeast. *Nature* **459**:253-256 (2009).
- 561
- 562 11. J. H. Koschwanez, K. R. Foster, & A. W. Murray. Sucrose utilization in budding yeast as a
563 model for the origin of undifferentiated multicellularity. *PLoS Biol.* **9**:e1001122 (2011)
564

- 565 12. J. H. Koschwanez, K. R. Foster, & A. W. Murray. Improved used of a public good selects for
566 the evolution of undifferentiated multicellularity. *eLife* **2**:e00367 (2013).
567
- 568 13. C. Ratzke, J. Denk, & J. Gore. Ecological suicide in microbes. *Nat. Ecol. Evol.* **2**:867-872
569 (2018).
570
- 571 14. J. Postmus *et al.*, Quantitative analysis of the high temperature-induced glycolytic flux
572 increase in *Saccharomyces cerevisiae* reveals dominant metabolic regulation. *J. Biol. Chem.*
573 **283**:23524-23532 (2008).
574
- 575 15. R. M. Walsh, & P. A. Martin. Growth of *saccharomyces cerevisiae* and *saccharomyces*
576 *uvarum* in a temperature gradient incubator. *J. Inst. Brew.* **83**:169-172 (1977).
577
- 578 16. D. A. Ratkowsky, R. K. Lowry, T. A. McMeekin, A. N. Stokes, & R. E. Chandler. Model for
579 bacterial culture growth rate throughout the entire biokinetic temperature range. *J. Bacteriol.*
580 **154**:1222-1226 (1983).
581
- 582 17. E. Dekel, U. Alon. Optimality and evolutionary tuning of the expression level of a protein.
583 *Nature* **436**, 588-592 (2005).
584
- 585 18. M. Scott, & T. Hwa. Bacterial growth laws and their applications. *Curr Opin Biotechnol.*
586 **22**:559-565 (2011).
587
- 588 19. V. Bharathi *et al.* Use of *ade1* and *ade2* mutations for development of a versatile red/white
589 colour assay of amyloid-induced oxidative stress in *Saccharomyces cerevisiae*. *Yeast* **33**,
590 607-620 (2016).
591
- 592 20. N. Q. Balaban. Persistence: mechanisms for triggering and enhancing phenotypic variability.
593 *Curr. Opin. Genet. Dev.* **21**, 768-775 (2011).
594
- 595 21. H. C. Causton *et al.* Remodeling of yeast genome expression in response to environmental
596 changes. *Mol. Biol. Cell* **12**:323-337 (2001).
597

- 598 22. A. P. Gasch, *et al.* Genomic expression programs in the response of yeast cells to
599 environmental changes. *Mol. Biol. Cell* **11**:4241-4257 (2000).
600
- 601 23. K. Sugiyama, A. Kawamura, S. Izawa, & Y. Inoue. Role of glutathione in heat-shock-induced
602 cell death of *Saccharomyces cerevisiae*. *Biochem. J.* **352**:71-78 (2000).
603
- 604 24. K. Sugiyama, S. Izawa, & Y. Inoue. The Yap1p-dependent induction of glutathione synthesis
605 in heat shock response of *Saccharomyces cerevisiae*. *J. Biol. Chem.* **275**: 15535-15540
606 (2000).
607
- 608 25. J. F. Davidson, B. Whyte, P. H. Bissinger, & R. H. Schiestl. Oxidative stress is involved in
609 heat-induced cell death in *Saccharomyces cerevisiae*. *Proc Natl Acad Sci USA* **93**:5116-5121
610 (1996).
611
- 612 26. F. M. Yakes, & B. van Houten. Mitochondrial DNA damage is more extensive and persists
613 longer than nuclear DNA damage in human cells following oxidative stress. *Proc. Natl. Acad.*
614 *Sci. U.S.A.* **94**:514-519 (1997).
615
- 616 27. E. Cabiscol, E. Piulats, P. Echave, E. herrero, & J. Ros. Oxidative stress promotes specific
617 protein damage in *Saccharomyces cerevisiae*. *J. Biol. Chem.* **275**:27393-27398 (2000).
618
- 619 28. T. Bilinski, J. Litwinska, M. Blaszczyński, & A. Bajus. SOD deficiency and the toxicity of the
620 products of autoxidation of polyunsaturated fatty acids in yeast. *Biochim. Biophys. Acta.*
621 **1001**:102-106 (1989).
622
- 623 29. D. J. Jamieson. Oxidative stress responses of the yeast *Saccharomyces cerevisiae*. *Yeast*
624 **14**:1511-1527 (1998).
625
- 626 30. B. Zechmann *et al.* Subcellular distribution of glutathione and its dynamic changes under
627 oxidative stress in the yeast *Saccharomyces cerevisiae*. *FEMS Yeast Res* **11**:631-642 (2011).
628
- 629 31. C. Kumar *et al.* Glutathione revisited: a vital function in iron metabolism and ancillary role in
630 thiol-redox control. *EMBO J.* **30**:2044-2056 (2011).
631

- 632 32. M. B. Toledano, C. Kumar, N. Le Moan, D. Spector, & F. Tacnet. The system biology of thiol
633 redox system in Escherichia coli and yeast: differential functions in oxidative stress, iron
634 metabolism and DNA synthesis. *FEBS Lett* **581**:4549 (2007).
635
- 636 33. M. T. Elskens, C. J. Jaspers, & M. J. Penninckx. Glutathione as an endogenous sulfur source
637 in the yeast *Saccharomyces cerevisiae*. *J Gen Microbiol* **137**:637-644 (1991).
638
- 639 34. K. Mehdi, & M. J. Penninckx. An important role for glutathione and γ -glutamyltranspeptidase
640 in the supply of growth requirements during nitrogen starvation of the yeast *Saccharomyces*
641 *cerevisiae*. *Microbiology* **143**:1885-1889 (1997).
642
- 643 35. M. Thorsen *et al.* Glutathione serves an extracellular defence function to decrease arsenite
644 accumulation and toxicity in yeast. *Mol. Microbiol.* **84**:1177-1188 (2012).
645
- 646 36. G. G. Perrone, C. M. Grant, & I. W. Dawes. Genetic and environmental factors influencing
647 glutathione homeostasis in *Saccharomyces cerevisiae*. *Mol. Biol. Cell* **16**:218-230 (2005).
648
- 649 37. D. Giustarini *et al.* Pitfalls in the analysis of the physiological antioxidant glutathione (GSH)
650 and its disulphide (GSSG) in biological samples: An elephant in the room. *J. Chromatogr B*
651 *Analyt Technol Biomed Life Sci* **1019**:21-28 (2016).
652
- 653 38. A. R. Araujo, M. L. Saraiva, & J. L. Lima. Determination of total and oxidized glutathione in
654 human whole blood with a sequential injection analysis system. *Talanta* **74**:1511-1519 (2008).
655
- 656 39. C. M. Grant, F. H. MacIver, & I. W. Dawes. Glutathione is an essential metabolite required for
657 resistance to oxidative stress in the yeast *Saccharomyces cerevisiae*. *Curr Genet* **29**:511-515
658 (1996).
659
- 660 40. A. Bourbouloux, P. Shahi, A. Chakladar, S. Delrot, & A. K. Bachhawat. Hgt1p, a high affinity
661 glutathione transporter from the yeast *Saccharomyces cerevisiae*. *J. Biol Chem.*
662 **275**:13259-13265 (2000).
663
- 664 41. M. Dhaoui *et al.* Gex1 is a yeast glutathione exchanger that interferes with pH and redox
665 homeostasis. *Mol Biol Cell* **22**:2054-2067 (2011).

666
667 42. K. Kiriya, K. Y. Hara, & A. Kondo. Extracellular glutathione fermentation using engineered
668 *Saccharomyces cerevisiae* expressing a novel glutathione exporter. *Appl Microbiol Biotechnol*
669 **96**:1021-1027 (2012).
670
671 43. R. Green *et al.* Rapid evolution of an overt metabolic defect restores balanced growth. *BioRxiv*
672 doi.org/10.1101/498543 (2018).
673
674 44. L. Dai, D. Vorselen, K. Korolev, & J. Gore. Generic indicators for loss of resilience before a
675 tipping point leading to population collapse. *Science* **336**:1175-1177 (2012).
676
677 45. S. H. Strogatz. *Nonlinear dynamics and chaos: with applications to physics, biology,*
678 *chemistry, and engineering* (Westview, Boulder, CO, 1994).
679
680 46. M. Mojtahedi *et al.* Cell fate decision as high-dimensional critical state transition. *PLoS Biol*
681 **14**:e2000640 (2016).
682
683 47. J. Garcia-Ojalvo, J. M. Sancho, L. Ramirez-Piscina. A nonequilibrium phase transition with
684 colored noise. *Physics Letters A* **168**, 35-39 (1992).
685
686 48. H. Youk, W. A. Lim. Secreting and sensing the same molecule allows cells to achieve versatile
687 social behaviors. *Science* **343**,1242782 (2014).
688
689 49. C. Trapnell *et al.* Differential gene and transcript expression analysis of RNA-seq experiments
690 with TopHat and Cufflinks. *Nat. Protoc.* **7**, 562-578 (2012).
691
692 50. C. Riccardi, & I. Nicoletti. Analysis of apoptosis by propidium iodide staining and flow
693 cytometry. *Nat Prot* **1**:1458-1461 (2006).
694
695

696 **Supplemental Information:**

- 697 • Supplementary Figures 1-14
698 • Supplementary Text: Detailed description of the mathematical model

699

700 **Acknowledgements:**

701 We thank Shalev Itzkovitz and Arjun Raj for insightful comments on our manuscript. We also thank
702 the members of the Youk laboratory for helpful discussions and Mehran Mohebbi for help with
703 initial experiments. H.Y. was supported by the European Research Council (ERC) Starting Grant
704 (MultiCellSysBio, #677972), the Netherlands Organisation for Scientific Research (NWO) Vidi
705 award (#680-47-544), the CIFAR Azrieli Global Scholars Program, and the EMBO Young
706 Investigator Award.

707

708 **Author contributions:**

709 H.Y. initiated this research and performed the initial growth experiments. D.S.L.T. subsequently
710 designed additional experiments with guidance from H.Y.. D.S.L.T. performed all the experiments,
711 developed the mathematical model, and analysed the data with advice from H.Y.. D.S.L.T. and
712 H.Y. discussed and checked all the data and wrote the manuscript.

713

714 **DECLARATION OF INTERESTS**

715 The authors declare no competing interests.

716

717 **Figure captions:**

718

719 **Figure 1. Conventional, cell-autonomous view of temperature-dependent cell-replications.**

720 (a) The conventional view states that cells autonomously replicate at "habitable temperatures"
721 (blue region) and that at sufficiently high temperatures (i.e., "unlivable temperatures"), cells fail to
722 replicate and can eventually die (red region).

723 (b) Growth rate as a function of temperature for populations of wild-type yeast cells. Black data
724 points in the blue region are for populations with sustained, exponential growth over time and
725 white data points in the red region are for populations without sustained exponential growth (error
726 bars represent the mean with s.e.m., n = 3 replicates per data point). 39 °C is near a boundary of
727 blue and red regions. (Also see Supplementary Fig. 1).

728 (c) The conventional view (explained in (a)) applied to budding yeast, based on the data in (b).

729 (d) Question that we investigated in our study: can microbes collectively combat rising
730 temperatures so that they can turn a temperature that is unlivable (e.g., 40 °C shown in (c)) into
731 a habitable temperature?

732

733

734 **Figure 2. Population-density determines replicability of cells and habitability of each**
735 **temperature.**

736 (a-c) Population-density (number of cells/mL) measured over time with a flow cytometer for
737 populations of wild-type yeast of differing initial population-densities at (a) a conventionally-defined
738 habitable temperature (38.4 °C), (b) near the edge of conventionally-defined habitable and
739 unlivable temperatures (39.2 °C), (c) and at a conventionally-defined unlivable temperature (40.3
740 °C). Figure 1b sets the conventional definition of temperature's habitability. For (a-b): Each color
741 shows n = 8 populations that start with the same density. Red curves show no growths beyond
742 initial transient growths (i.e., "no growth"). Green curves show unpredictable growths (i.e., "random
743 growth"). Blue curves show deterministic, exponential growths whereby all populations identically
744 grow (i.e., "deterministic growth"). For (c): Each color shows n = 4 populations with the same initial
745 population-density. All colors except the red show growths by ~10-fold.

746 (d) Phase diagram constructed from measurements. Colors of regions and triangles represent the
747 behaviors mentioned in (b) - blue marks deterministic growth, green marks random-growth, red
748 marks no-growth, and grey marks populations not growing as they have more cells than the
749 carrying capacity. Each triangle represents an experiment of the type shown in (a-c). (Also see
750 Supplementary Figs. 3-4 for details).

751 (e) Growth rates of populations in the no-growth phase (red), random-growth phase (green) and
752 deterministic-growth phase (blue) as a function of temperature (error bars represent the mean with
753 s.e.m., $n = 6$ or more replicates per data point for temperatures below $40\text{ }^{\circ}\text{C}$, and $n = 3$ for
754 temperatures above $40\text{ }^{\circ}\text{C}$). Grey data are from Figure 1b.

755 (f) Phase diagrams constructed for engineered yeast strains that constitutively express *GFP* at
756 the indicated levels (1x and 100x). Triangles indicate experimental data. Since the wild-type
757 strain's genetic background is slightly different from that of GFP-expressing strains, compare the
758 1x-GFP strain with the 100x-GFP strain only. (Also see Supplementary Fig. 5).

759

760

761 **Figure 3. Cells collectively combat death to avoid extinction high temperatures.**

762 (a) The number of survivors/mL (circles) over time in a non-growing wild-type population at 41.0
763 $^{\circ}\text{C}$. Brown line is an exponentially decaying function fitted to the first three data points (between
764 10 and 40 hours). Blue curve is a power-law function fitted to the same data points. (Also see
765 Supplementary Fig. 6).

766 (b) Number of survivors/mL for three populations of differing initial population-densities at $41.0\text{ }^{\circ}\text{C}$
767 measured as in (a). Initial population-densities, after transient growths, are 92,000 cells/mL
768 (purple), 231,000 cells/mL (orange), and 312,000 cells/mL (blue). Dashed lines represent an
769 exponentially decreasing function fitted to the first three time points. (Also see Supplementary Fig.
770 6).

771 (c) Cartoon illustrating the conventional view which states that cells autonomously die and that
772 every cell has the same probability of dying per unit time. This means that the population half-life
773 is independent of the initial population-density for every temperature. Different colors represent
774 different temperatures as indicated.

775 (d) Population half-life as a function of initial population-density, based on fitting an exponentially
776 decreasing function to the number of survivors/mL measured during the first 24 hours of incubation
777 (after ~ 20 hours of transient growths due to cells coming from $30\text{ }^{\circ}\text{C}$ and adjusting to the new
778 temperature). Shown here are the half-lives of populations at $39.2\text{ }^{\circ}\text{C}$, $40\text{ }^{\circ}\text{C}$, $40.3\text{ }^{\circ}\text{C}$, $40.8\text{ }^{\circ}\text{C}$,
779 $42\text{ }^{\circ}\text{C}$, and $43\text{ }^{\circ}\text{C}$, each in a different color as indicated (error bars represent the mean with s.e.m.,
780 $n = 3$ replicates per data point). Circles represent populations in the no-growth phase. The two
781 squares (at $39.2\text{ }^{\circ}\text{C}$ and $40\text{ }^{\circ}\text{C}$) represent populations that grew due to having sufficient
782 population-densities to trigger their own growths (see Fig. 2d).

783

784

785 **Figure 4. Cells secrete and extracellularly accumulate glutathione to help each other and**
786 **future generations of cells replicate at high temperatures.**

787 (a) Schematic description of experiments in (b) and (c) to determine whether (“1”) intracellular or
788 (“2”) extracellular factors dictate population growth.

789 (b) At 39.2 °C. Labelled “1” in (a): wild-type cells were transferred (boxed data point) from log-
790 phase populations (blue, initially ~10.000 cells/mL) to fresh media (green, initially ~400 cells/mL).
791 Each color shows n = 4 replicate populations. (Also see Supplementary Fig. 7).

792 (c) At 39.2 °C. Labelled “2” in (a): fresh cells from 30 °C were incubated in a growth medium that
793 previously harbored log-phase cells at ~39 °C for 0 hours (grey), 12 hours (red), or 16 hours
794 (purple). Each color shows at least n = 6 replicate populations. (Also see Supplementary Fig. 8).

795 (d) No-growth populations (initially ~400 cells/mL) at 39.2 °C. Adding either ascorbic acid (5 mM
796 - yellow) or glutathione (200 μM - green) to the growth media induces population growths. Without
797 adding either one, populations do not grow (grey). Each color shows n = 4 replicate populations.

798 (e) At 39.2 °C. The measured concentrations of extracellular glutathione as a function of the
799 population-density over time for no-growth (red, initially ~400 cells/mL), random-growth (light blue,
800 initially ~2,000 cells/mL), and deterministic-growth populations (dark blue, initially ~10,000
801 cells/mL) (error bars represent the mean with s.e.m., n = 3 replicates per data point). The arrow
802 shows both the population-density and concentration of extracellular glutathione increasing
803 together over time. (Also see Supplementary Fig. 11).

804 (f) At 39.2 °C. Sensitivity of no-growth populations (initially ~400 cells/mL) to glutathione added
805 into the growth medium, as a function of glutathione concentration (error bars represent the mean
806 with s.e.m., n = 4 replicates per data point). Shown here is the fold-change in the population-
807 density after two days of incubation.

808 (g) Cartoon illustrating the mechanism deduced in (a-f). Yeasts secrete and extracellularly
809 accumulate glutathione at high temperatures, inducing population growth when its concentration
810 reaches at least a threshold amount (~0.3 μM from (f)).

811

812

813 **Figure 5. Mathematical model with one free parameter recapitulates all the main**
814 **experimental data.**

815 (a-b) Description of the mathematical model (see full description in the Supplementary text). (a) A
816 cell (yellow circle) can be in three states. In each time step, any alive cell either stays alive without
817 replicating, replicates, or dies. Alive cells constantly secrete glutathione (green circle). (b)
818 Schematic description of the probabilities that describe each of the transitions between states

819 shown in (a). Left panel: probability of a cell dying (red line) is fixed by the temperature and does
820 not change over time. It linearly increases with temperature and, beyond some temperature, it
821 exceeds the maximum allowed value for the probability of a cell replicating (grey line). Right panel:
822 probability of a cell replicating (blue curve) non-linearly increases with the concentration of the
823 extracellular glutathione.

824 (c-f) Results generated by the model described in (a-b) with a single fixed set of parameters for
825 all the panels. Model recapitulates: (c) the population-growth curves (compare with Fig. 2a), (d)
826 the phase diagram (compare with Fig. 2d), (e) population-density dependent deaths (compare
827 with Fig. 3b), (f) population half-life (based on cell deaths during the first day of incubation -
828 compare with Figure 3d), the number of survivors decaying over time as a heavy-tailed function
829 (see Supplementary Fig. 12), and single-cell-level data on growths (compare Extended Data Fig.
830 1 with Extended Data Fig. 3). The number of replicate simulations matches that of the respective
831 experiments. (Also see Supplementary Fig. 12).

832

833

834 **Figure 6. Budding yeast exports glutathione whose extracellular role – not intracellular**
835 **roles - as antioxidant enables yeasts to survive high temperatures.**

836 (a) At 39.2 °C. Wild-type populations (all initially ~20,000 cells/mL) that should deterministically
837 grow if left alone. A masking agent (M2VP) that inactivates extracellular glutathione was added
838 after 4.5 hours (dark brown) or 8.5 hours (light brown) of incubation. Grey curve shows populations
839 that did not receive the masking reagent. Each color shows n = 4 replicate populations. (Also see
840 Supplementary Fig. 13).

841 (b) Schematic showing how the budding yeast synthesizes, imports, and exports glutathione.
842 Glutathione is intracellularly synthesized via an enzyme encoded by *GSH1*. Glutathione is
843 imported by a proton-coupled glutathione-importer encoded by *HGT1*. Glutathione is exported by
844 numerous exporters (not all shown), including proton antiporters encoded by *GEX1,2* and an ATP-
845 dependent exporter encoded by *ADP1*.

846 (c) At 39.2 °C. Light blue curves show deterministically growing populations of a mutant strain
847 (*hgt1Δ*-strain) that cannot import glutathione (initially ~10,000 cells/mL). Grey curves show mutant
848 populations (initially ~400 cells/mL) incubated without any glutathione added. Dark blue curves
849 show mutant populations (initially ~400 cells/mL) incubated with 250 μM of glutathione added to
850 the media. Each color shows n = 4 replicate populations.

851 (d) At 39.2 °C. Populations of a mutant strain that lacks some of the main glutathione exporters
852 (*gex1,2Δ-adp1Δ*-strain) (initially ~9,500 cells/mL (purple) or ~7,500 cells/mL (pink)). Wild-type

853 populations shown as a comparison (grey, initially ~9,500 cells/mL). Each color shows n = 4
854 replicate populations. (Also see Extended Data Fig. 4).

855 (e) At 41 °C. Wild-type populations of various initial densities (from ~400 cells/mL (lightest green
856 curves) to ~14,000 cells/mL (darkest green curves)) grown in media supplemented by 750 μM of
857 glutathione. Each color shows at least n = 3 replicate populations.

858 (f) Cartoon illustrating mechanisms deduced in (a-e). Exporting glutathione is necessary and
859 sufficient for yeasts to reshape the habitability of temperature. For yeasts to survive and replicate
860 at high temperatures, extracellular glutathione is (1) necessary since blocking glutathione or
861 blocking glutathione-export stops yeast's growths and is (2) sufficient since adding glutathione or
862 blocking glutathione-import enables yeasts to grow.

863

864

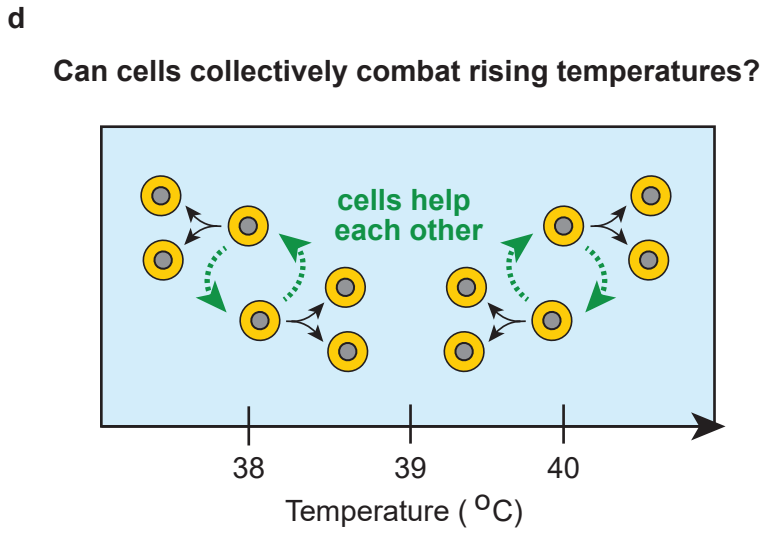
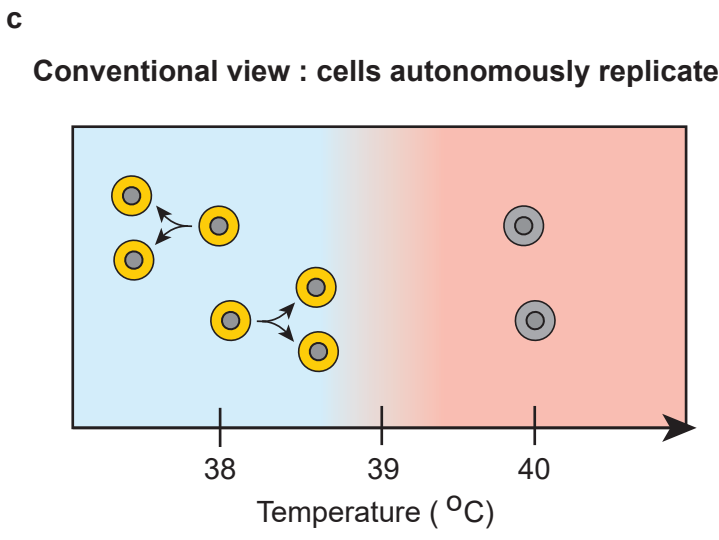
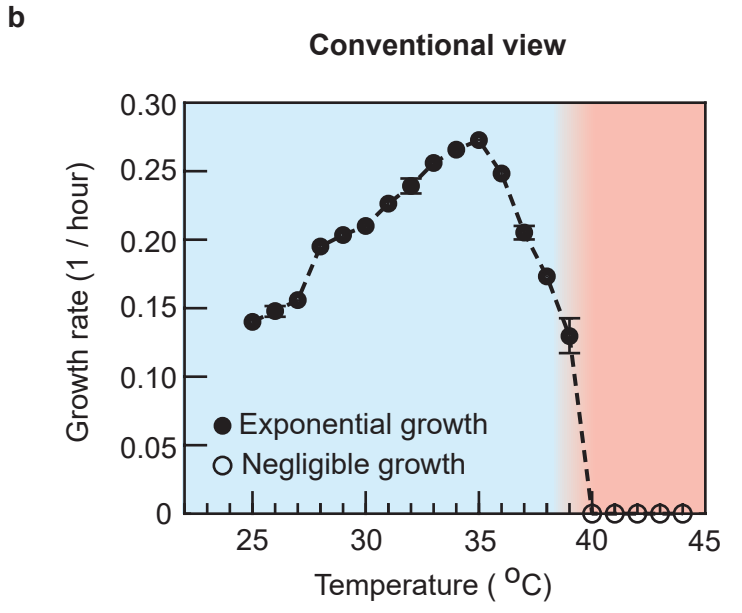
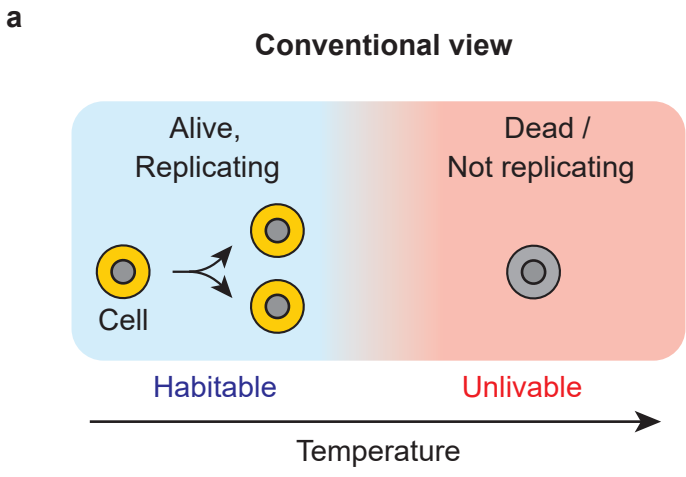


Fig. 1

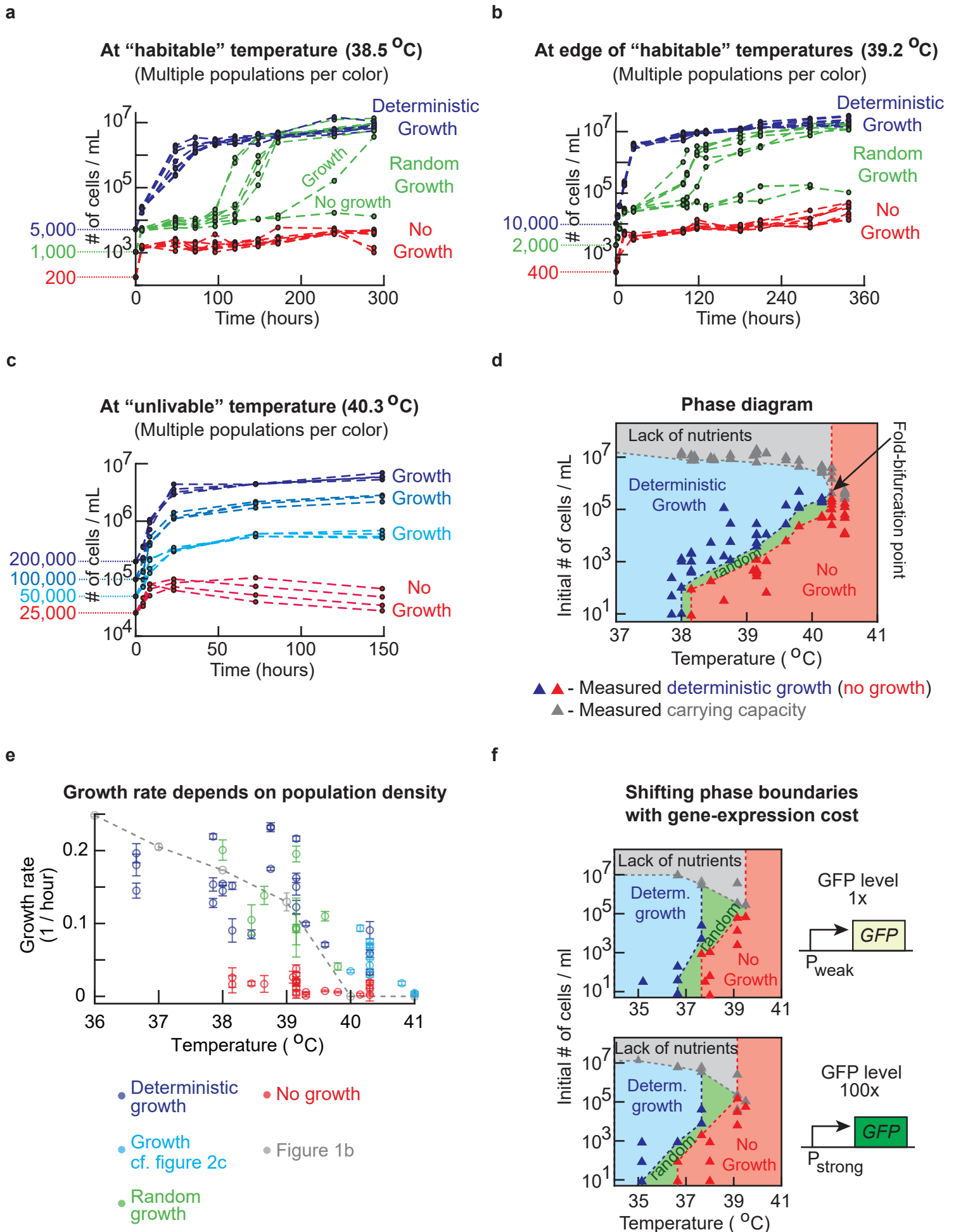
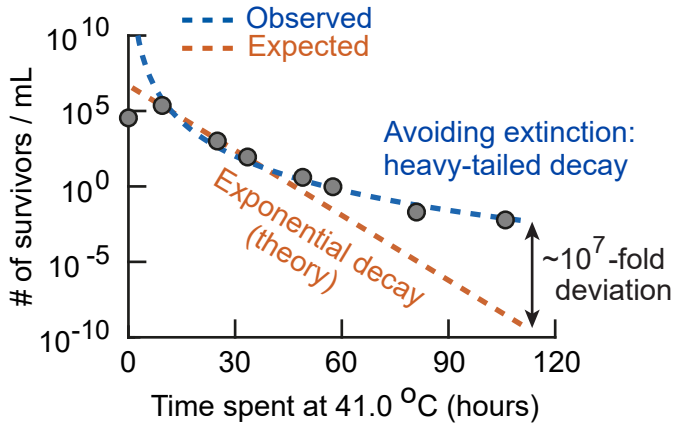


Fig. 2

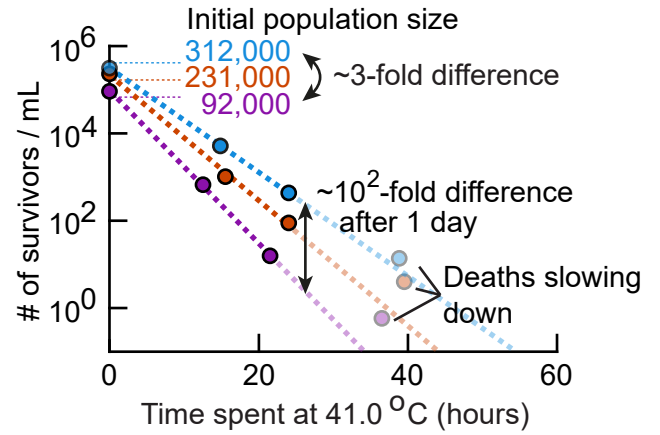
a

Vastly more cells survive than expected at high temperatures



b

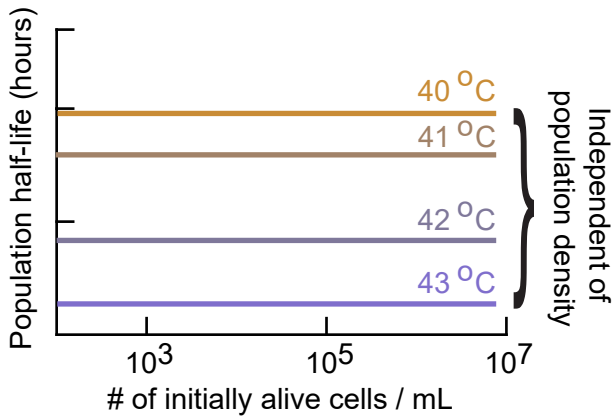
Larger populations initially die more slowly (During first 24 hours)



(c-d) Time taken for # of survivors to be halved

c

Conventional theory:
cells autonomously die



d

Experiment

(Based on initial death-rate, before heavy-tailed decay)

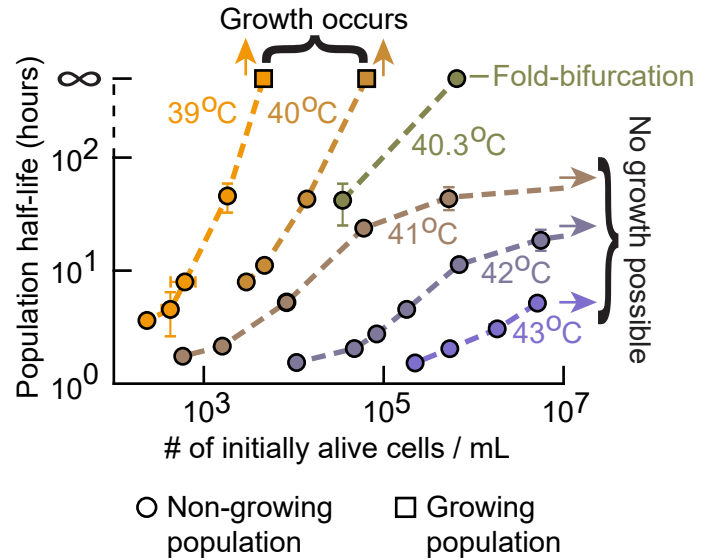


Fig. 3

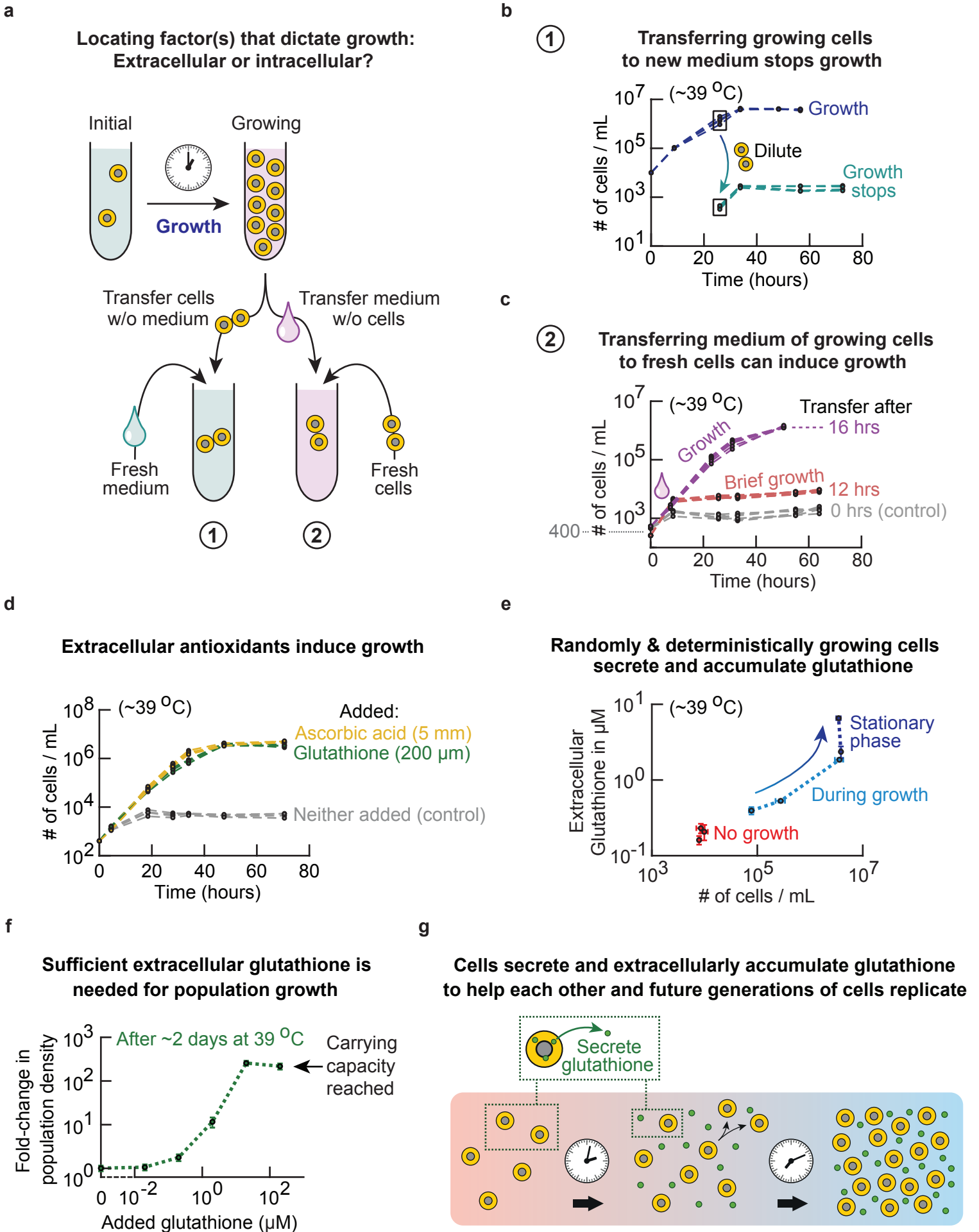
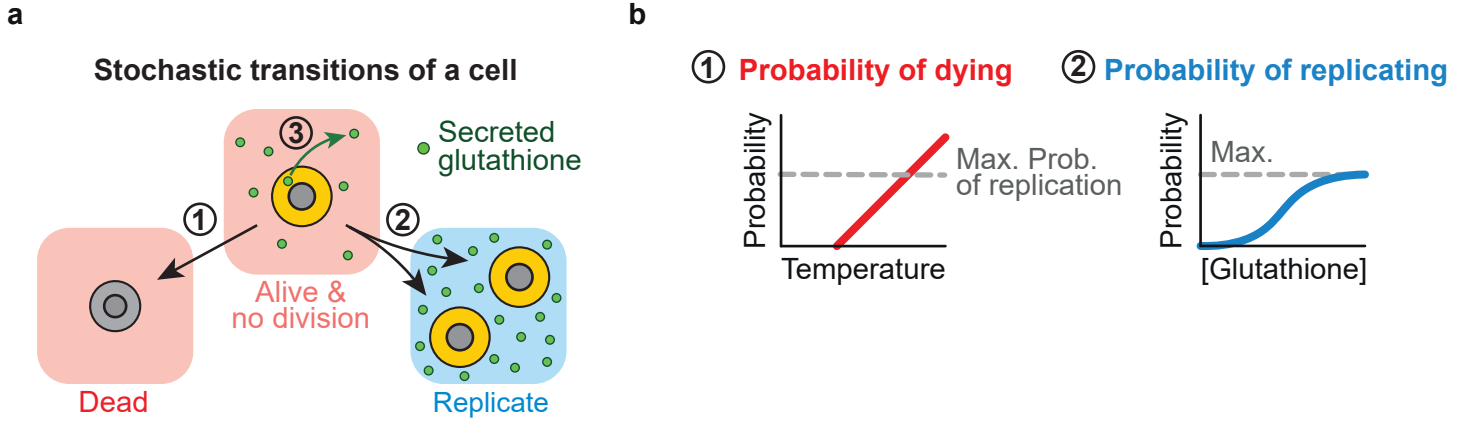


Fig. 4

Mathematical model: schematics



Mathematical model recapitulates key features

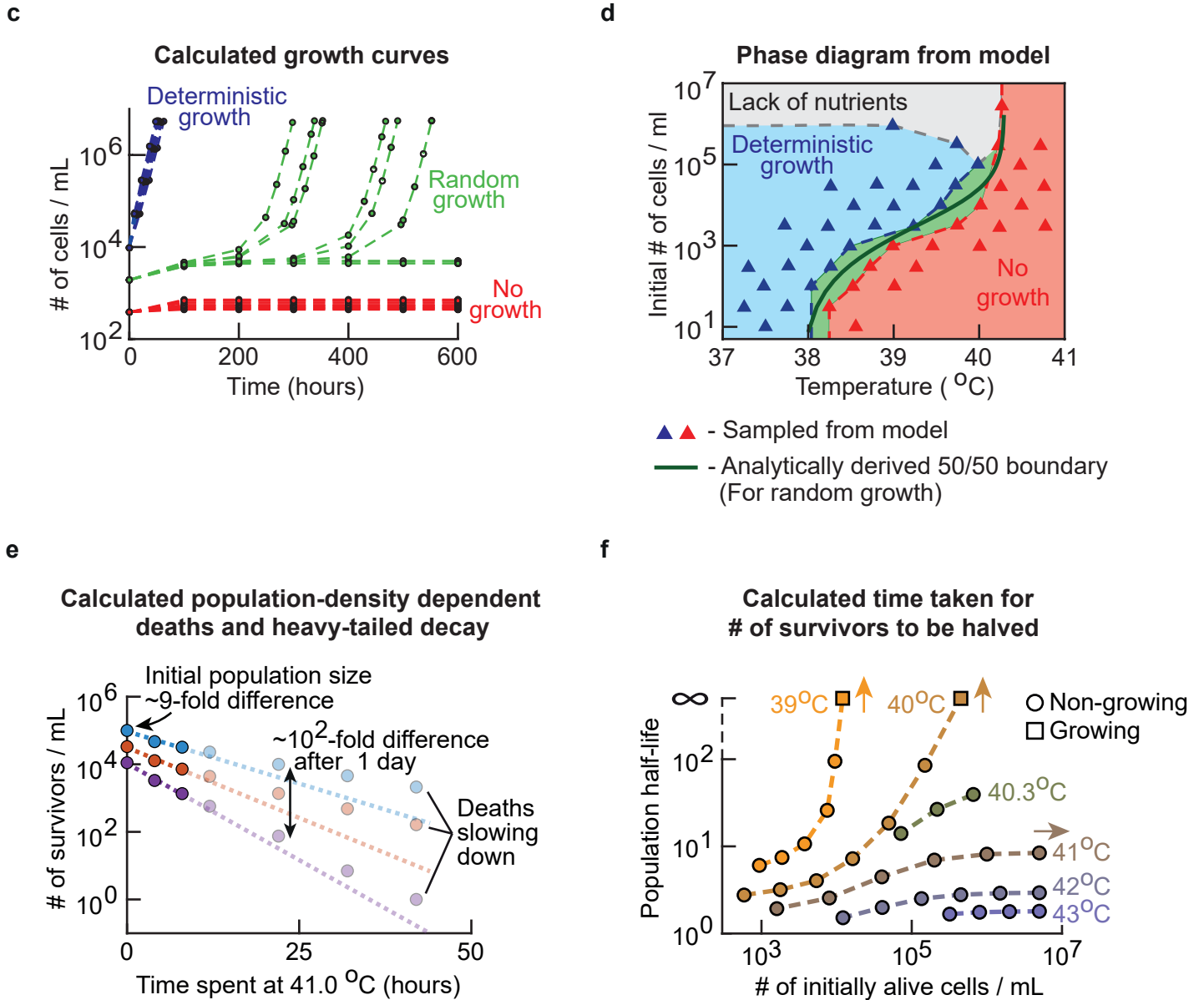
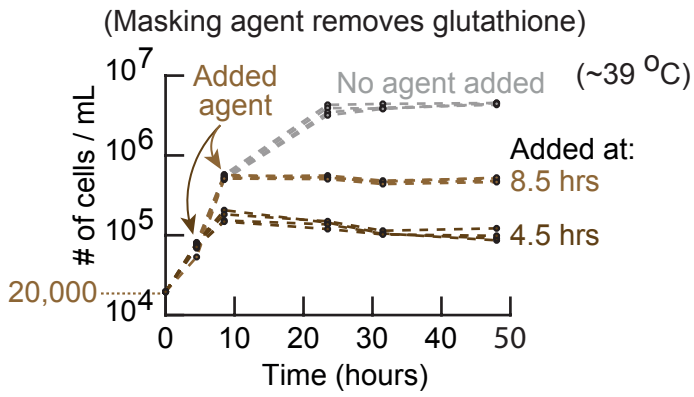
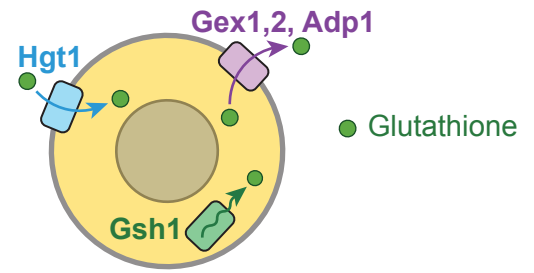


Fig. 5

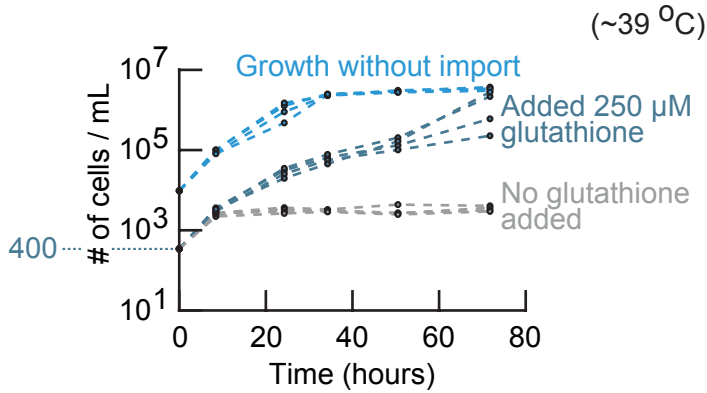
a Removing extracellular glutathione stops growth



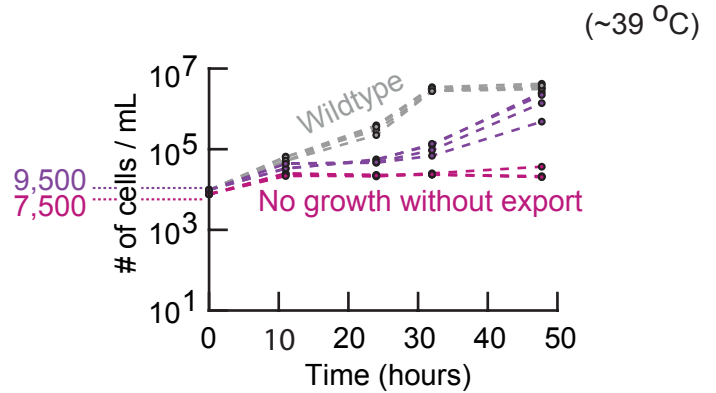
b Schematic: glutathione synthesis & transport



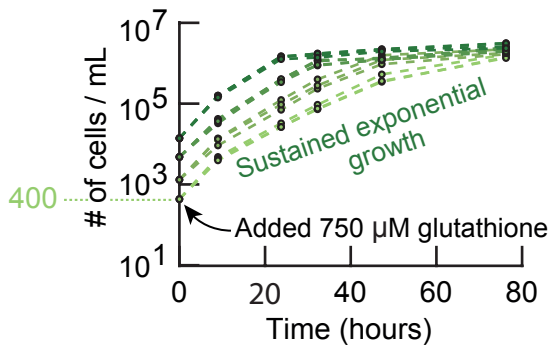
c Populations that cannot import glutathione can grow (*hgt1Δ*)



d Populations that cannot export glutathione cannot grow (*gex1,2Δ, adp1Δ*)



e Growth enabled at 'forbidden' temperature (41 °C) by adding extracellular glutathione



f Exporting glutathione is necessary & sufficient for making temperature habitable

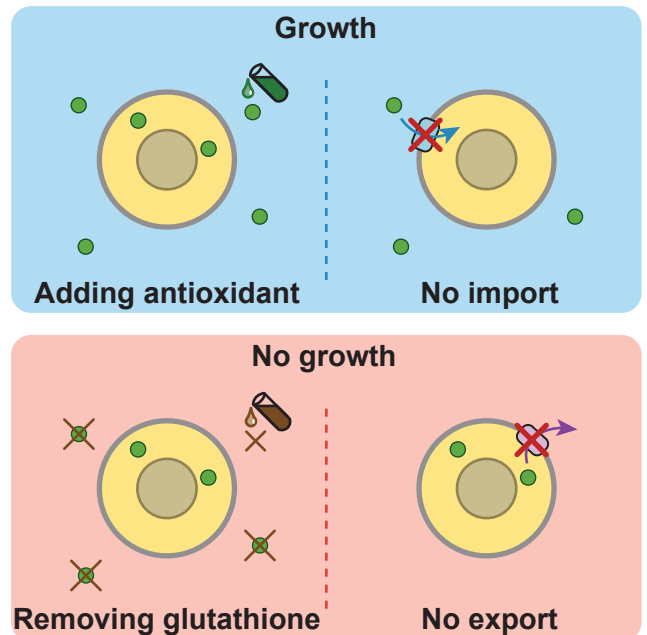


Fig. 6